Polymer Journal
https://doi.org/10.1038/s41428-024-00901-0

ORIGINAL ARTICLE

# Construction of peptide/plasmid DNA complexes for plant gene transfection via the basic leucine zipper domain

Kota Nomura[1] · Seiya Fujita[1] · Yuki Shimatani[1] · Taichi Kurita[1] · Chonprakun Thagun[1] · Naoya Abe[1] · Kazusato Oikawa[1] · Kousuke Tsuchiya[1,2] · Hirotaka Uji[1] · Keiji Numata[1,2,3]

Received: 28 December 2023 / Revised: 31 January 2024 / Accepted: 6 February 2024


## Abstract

An important method for plant genetic modification is using peptide/pDNA complexes to transfer genes into plant cells. With conventional carrier peptides, the peptide sequence must contain a high amount of cationic amino acids to condense and introduce pDNA. As a result, the dissociation of pDNA from the complex is inefficient, often causing problems. Herein, we designed a new peptide carrier that mimics the basic leucine zipper (bZIP) domain of DNA-binding proteins, in which $(LU)_4$ is the leucine zipper motif and $(KUA)_3$ is the basic DNA-binding and cell-penetrating motif (U = α-aminoisobutyric acid). After $(KUA)_3$-$(LU)_4$ peptide was mixed with pDNA, DNA molecules were condensed to form nanoparticles of approximately 130 nm. Furthermore, when complexes of $(KUA)_3$-$(LU)_4$ peptide and pDNA were introduced into the leaves of *Arabidopsis thaliana* (*A. thaliana*), expression of the reporter protein was detected in the plant cells. Thus, $(KUA)_3$-$(LU)_4$ peptide that mimics the bZIP domain is a novel and efficient carrier for pDNA with high dissociation efficiency.

## Introduction

Researchers have significantly focused on plant genome engineering because the strategy can be used to produce plants with high functionality, contributing to sustainable development goals [1, 2]. Gene transfer methods, such as Agrobacterium-mediated transformation, biolistic particle-projectile bombardment, and polyethylene glycol (PEG)-based membrane fusion, have been extensively studied to rapidly and efficiently transform exogenous DNA fragments (which harbor gene expression cassettes that contain biomolecules of interest) into plant genomes [3, 4]. Nanoparticle delivery systems that use carrier molecules and cargo DNA complexes, such as DNA nanostructures [5], carbon nanotubes (CNTs) [6, 7], and peptides [8–10], have been extensively developed. In recent years, researchers have increasingly focused on genetically modifying plants with a functional peptide, as this strategy can easily impart functions such as organelle selectivity and endosomal escape ability [11, 12]. The peptide approach involves condensing plasmid DNA (pDNA) into ionic complexes. These complexes are formed with a cationic peptide sequence that contains two functional domains. The first domain includes a translocating peptide, such as a cell membrane permeation sequence and an endosomal escape domain [13], along with an organelle target sequence [14, 15]. The second domain is a DNA-binding domain that typically contains a tandem sequence of positively charged amino acids. This method efficiently transports pDNA to animal and plant cells. For example, $(KH)_9$-BP100, which is a conjugate of the cell-penetrating peptide (CPP) BP100 [16] and the condensed DNA sequence $(KH)_9$ [17], condenses pDNA to form complexes of approximately 100 nm. Furthermore, this complex efficiently permeates the cell membrane and is transported into the cell through the BP100 sequence [8]. However, these cationic polypeptides perform genetic modifications with a relatively low

**Supplementary information** The online version contains supplementary material available at https://doi.org/10.1038/s41428-024-00901-0.

✉ Keiji Numata
numata.keiji.3n@kyoto-u.ac.jp

[1] Department of Material Chemistry, Graduate School of Engineering, Kyoto University, Kyoto Daigaku Katsura, Nishikyo-ku, Kyoto 615-8510, Japan

[2] Biomacromolecules Research Team, RIKEN Center for Sustainable Resource Science, 2-1 Hirosawa, Wako, Saitama 351-0198, Japan

[3] Institute for Advanced Biosciences, Keio University, Nipponkoku 403-1, Daihouji, Tsuruoka, Yamagata 997-0017, Japan

Published online: 05 March 2024

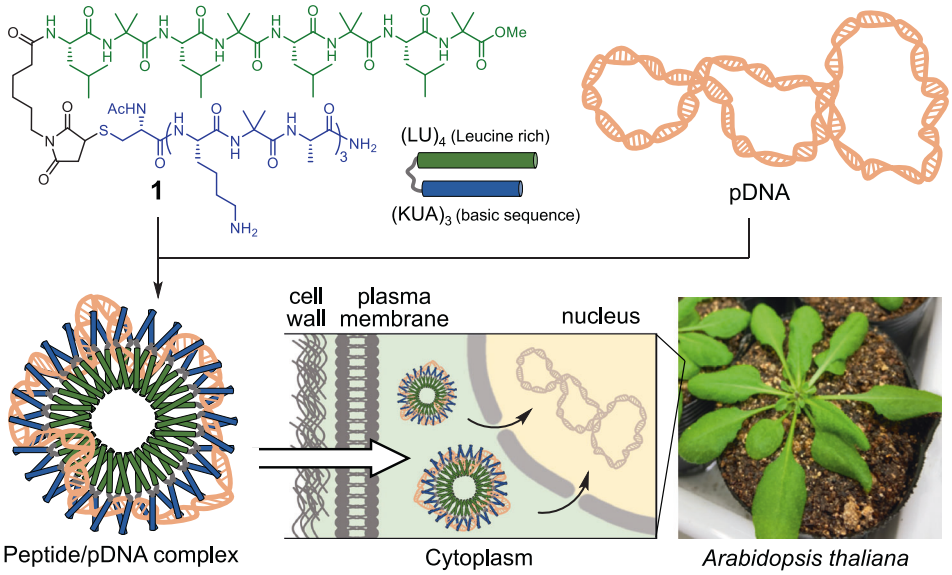


**Fig. 1** Chemical structures of bZIP mimicking peptide $(KUA)_3$-$(LU)_4$ **1**. Schematic illustration of pDNA delivery into plants using a peptide/pDNA complex

efficiency due to the strong electrostatic interaction between pDNA and peptides, which inhibits the dissociation of pDNA from the complex [18–21]. Therefore, it is necessary to develop peptide/pDNA complexes without strong electrostatic interactions to improve the efficiency of target protein expression.

In nature, a motif called the basic leucine zipper (bZIP) domain binds DNA molecules [22, 23]. This bZIP motif is formed by two helices that contain a leucine-rich sequence and a cationic sequence. The cationic basic sequence interacts with DNA [22], and the leucine-rich sequence forms a dimeric coiled coil helical structure by hydrophobic interactions [24]. It is known that this coiled-coil structure facilitates the binding between cationic amino acids in the bZIP domain and DNA due to its helical rigidity. For example, the transcription factor GCN4 binds strongly to DNA even though only three cationic amino acids are available for DNA binding [25]. Using the coiled-coil helical bZIP motif as a DNA condensing peptide, it is possible to construct peptide carriers that contain fewer cationic amino acids and exhibit high dissociation efficiency in the cell for DNA delivery.

Various artificial helical peptides have been designed and chemically synthesized [26, 27]. One strategy is to introduce α-aminoisobutyric acid (Aib, U) into the peptide sequence [28, 29]. The Aib residue in peptides induces the formation of α- and $3^{10}$-helices due to steric repulsion between the α,α-dimethyl groups. Kimura et al. reported that helical peptides are composed of a repeating sequence that includes leucine (Leu, L) and Aib [30–32]. Amphipathic helical peptides composed of Leu-Aib (LU) can form various assemblies, such as micelles and vesicles, through hydrophobic interactions with aligned leucine residues. Additionally, we developed a CPP, $(Lys\text{-}Aib\text{-}Ala)_3$ ($(KUA)_3$), which contains an Aib residue that stabilizes the helical conformation [33]. These CPPs exhibit robust cell membrane permeability in animals and plants. Recently, we successfully delivered protein and pDNA molecules to plants using micelles and vesicles modified with these peptides [13, 34, 35].

Based on this background, herein, we utilized the bZIP domain-mimicking peptide as a new DNA binding domain that can form peptide/DNA complexes with modest dissociation efficiency. This peptide contains $(LU)_4$ and $(KUA)_3$ sequences and effectively condensed pDNA to form a nanoparticle of 130 nm. By treating plants with this peptide/pDNA complex, we successfully delivered exogenous genes into plant cells (Fig. 1). Therefore, bZIP-mimicking peptides may be promising carriers for pDNA.

## Materials and methods/Experimental procedure

### Materials

N-(6-maleimidocaproyloxy)sulfosuccinimide sodium salt (sulfo-EMCS) was purchased from Dojindo Laboratories (Kumamoto, Japan). Other chemicals were purchased from FUJIFILM Wako Pure Chemical Co. (Osaka, Japan). Ac-CKUAKUAKUA-$NH_2$ (Ac-C$(KUA)_3$-$NH_2$) **2** (HRMS and analytical HPLC results are shown in Supplementary Fig. S1) was purchased from the Research Resources Division of the RIKEN Center for Brain Science (Wako, Japan). Boc-LULULULU-OMe (Boc-$(LU)_4$-OMe) **3** was synthesized via liquid-phase peptide synthesis as described in previous studies [36, 37]. The purity of each peptide was >95%, as determined by reverse-phase high-performance liquid chromatography.

## Characterization and purification procedures

$^1$H NMR spectra were measured using a Bruker DPX-400 NMR spectrometer (Bruker Biospin, Rheinstetten, Germany) at 25 °C and 400 MHz. $D_2O$ was used as the NMR solvent. Mass spectrometry was conducted using MALDI-TOF mass spectrometry (Bruker ultrafleXtreme MALDI-TOF mass spectrometer, Bruker Daltonics GmbH & Co. KG, Bremen, Germany). Peptide purification was conducted with a Shimadzu Corporation HPLC system consisting of an autosampler SIL-20AC, a gradient pump LC-20AD, a column oven CTO-20AC, a UV/vis detector SPD-M20A, and a COSMOSIL C18-MS packed column (5 μm, 46 mm i.d. ×150 mm; Nacalai Tesque, Inc., Kyoto, Japan).

## Synthesis of $(KUA)_3$-$(LU)_4$ 1

The N-terminal Boc group of Boc-$(LU)_4$-OMe **3** was removed by treatment with HCl (4.0 M) in dioxane (Supplementary Scheme S1). The deprotected residue **4** (11 mg, 13 μmol) was then coupled with N-(6-maleimidocaproyloxy)sulfosuccinimide sodium salt (sulfo-EMCS, 18 mg, 44 μmol) using triethylamine (TEA, 3.7 μL, 27 μmol) in dry N,N-dimethylformamide (DMF). The reaction mixture was dried *in vacuo* and dissolved in dichloromethane, and the excess sulfo-EMCS was removed by washing with 4 wt% $KHSO_4$ aq. to yield the maleimide-functionalized $(LU)_4$ peptide (Mal-$(LU)_4$) **5**, which was used in the next reaction without any further purification. Compound **2** (4.2 mg, 4.1 μmol) and Compound **5** were conjugated via Michael addition with TEA (3.7 μL, 27 μmol). The reaction mixture was purified by HPLC to afford Compound **1** ($(KUA)_3$-$(LU)_4$, 2.2 mg, 1.1 μmol, 27%, purity: 91.0%), and the structure was confirmed by MALDI-TOF mass spectrometry and $^1$H-NMR spectroscopy (Supplementary Fig. S1). HRMS (MALDI+): calc. m/z for $[C_{95}H_{169}N_{23}O_{23}S + H]^+ = 2033.2561$; found = 2033.2880. $^1$H NMR (400 MHz, $D_2O$, δ): 0.85–0.96 (m, 24H, Leu C$^{\delta}H_3$), 1.30–1.84 (m, 87H, Ala C$^{\beta}H_3$, Aib C$^{\beta}H_3$, Lys C$^{\beta}H_2$, Lys C$^{\gamma}H_2$, Lys C$^{\delta}H_2$, mal-NCH$_2$C$H_2$, Mal-NCH$_2$CH$_2$C$H_2$, mal-NCH$_2$CH$_2$CH$_2$C$H_2$, Leu C$^{\beta}H_2$, Leu C$^{\gamma}H$), 2.05 (s, 3H, Ac), 2.29–2.33 (t, 2H, Mal-NCH$_2$CH$_2$CH$_2$CH$_2$C$H_2$), 2.63–2.70 (dd, 2H, mal-CHC$H_2$), 3.00–3.01 (m, 6H, Lys C$^{\epsilon}H_2$), 3.18–3.24 (dd, 2H, Cys C$^{\beta}H_2$), 3.30–3.35 (t, 1H, Mal-C$H$CH$_2$), 3.48–3.52 (t, 2H, mal-NC$H_2$), 3.72 (s, 3H, OMe), 4.13–4.26 (m, 10H, Ala C$^{\alpha}H$, Lys C$^{\alpha}H$, Leu C$^{\alpha}H$), 4.55–4.59 (t, 1H, Cys C$^{\alpha}H$).

## Preparation of peptide/pDNA complexes at various N/P ratios

The pDNA (p35S-NLuc-tNOS) used in this study encoded an engineered *Oplophorus* luciferase (NLuc) gene with the cauliflower mosaic virus 35S promoter and the *Agrobacterium tumefaciens* nopaline synthase gene terminator. Aqueous solutions of $(KUA)_3$-$(LU)_4$ **1** or $(KUA)_3$ **2** (13.5, 27, 54, 270 μM) were diluted with Milli-Q water and then mixed with pDNA aqueous solution (20 nM) at various N/P ratios (defined as the molar ratio of cationic peptide nitrogen to anionic pDNA phosphate). After that, the mixture was vortexed for 20 s and incubated at 25 °C for 30 min.

## Evaluation of peptide binding to pDNA by gel shift electrophoresis

Next, 2.5 μL of the peptide solution was incubated with pDNA (p35S-NLuc-tNOS) for 30 min, mixed with loading buffer, analyzed on a 1% agarose gel in TAE buffer and stained with ethidium bromide.

## Dynamic light scattering (DLS)

DLS and zeta potential measurements of the peptide assembly and the peptide/pDNA complexes were performed using a Zetasizer Nano ZS instrument (Malvern Instruments Ltd., Worcestershire, UK). These measurements were performed with peptide/pDNA complex solutions (800 μL) in a plastic cell (DTS1070) using a 633 nm He–Ne laser at 25 °C with a backscatter detection angle of 173° to estimate the hydrodynamic diameter as a Z-average size and polydispersity index (PDI). Each measurement was performed three times, and the resulting data were averaged to determine the standard deviation.

## Circular dichroism (CD) spectroscopy

CD measurements were attained with a JASCO J-1500 CD spectrometer (JASCO, Tokyo, Japan) at 25 °C. The measurements were taken in a quartz cell with a path length of 0.1 cm. Each CD spectrum was an average of 8 scans from 190 to 270 nm, with a 0.2 nm resolution, and was obtained at 100 nm/min with a bandwidth of 1 nm. A background CD spectrum of the solvent was obtained with Milli-Q water. The zeta potential and zeta deviation of the samples were measured three times with a zeta potentiometer, and the averaged data were obtained using Zetasizer software version 6.20 (Malvern Instruments, Ltd.).

## Atomic force microscopy (AFM) observation

For AFM measurements, sample solutions (5 μL) were spotted onto a cleaved mica surface. The solution on the mica surface was quickly frozen with dry ice and dried in vacuo. The dried samples were then observed under an ambient atmosphere at 25 °C using a Bruker Multimode 8 atomic force microscope (Bruker, Santa Barbara, CA) with

a cantilever (SCANASYST-AIR-HR, Bruker, Al reflective coating, 0.4 N/m, 130 kHz) in Peak Force QNM mode.

### Internalization of peptide/pDNA complexes into plants

*A. thaliana* seeds were germinated in pots with a planting medium consisting of soil (Promix, Rivière-du-Loup, Canada) and vermiculite at a ratio of 2:1 (v/v). The plants were grown in a plant incubator (Biotron NK System, Japan) under 12 h-day/12 h-night cycles at 23 °C and 65% relative humidity with a light intensity ranging from 100 to 130 μmol/$m^2$s. After 4-5 weeks of incubation after germination, plants with several expanded leaves were used for the experiments. To evaluate the internalization of pDNA (p35S-NLuc-tNOS) into plants, two peptide/pDNA complexes and two control samples were prepared in Milli-Q water: $(KUA)_3$-$(LU)_4$ (**1**)/pDNA complex, $(KUA)_3$ (**2**)/pDNA complex, $(KUA)_3$-$(LU)_4$ (**1**) (27 μM), and pDNA (10 nM). *A. thaliana* leaves were infiltrated with sample solutions of 100 μL/leave maximum using a needleless syringe onto the abaxial (backside) surface of the leaves [15]. The infiltrated plants were incubated for 14 h in the plant incubator for microscopy observations or 4 to 24 h for the luciferase assay.

### Confocal laser scanning microscopy (CLSM) observation

Cy3-labeled pDNA (p35S-NLuc-tNOS) was prepared with a Label IT Nucleic Acid Labeling Kit (Mirus Bio, LLC, Madison, WI). A peptide/pDNA complex (N/P = 1) was prepared from an aqueous solution of $(KUA)_3$-$(LU)_4$ (55 μM, 80 μL) and aqueous solution of Cy3-labeled pDNA (20 nM, 80 μL). *A. thaliana* leaves were infiltrated by the complex and incubated for 14 h. Afterward, the leaves were stained with calcofluor white (0.1 g/L) for 30 min and observed using CLSM with an LSM880 (Carl Zeiss, Oberkochen, Germany). CLSM images were acquired at excitation wavelengths of 405 nm for calcofluor white, 488 nm for chlorophyll, and 561 nm for Cy3 and visualized under a 63× oil-immersion objective.

### Evaluation of gene delivery efficiency in plants by Nano-Glo Luciferase assay

The infiltrated leaves were homogenized in *Renilla* Luciferase Assay Lysis Buffer (100 μL; Promega, Madison, WI). The lysate was centrifuged at 15,000 rpm at 4 °C for 10 min. The supernatant (50 μL) was added to a mixture (50 μL) of Nano-Glo Luciferase Assay Substrate (Promega) and Nano-Glo Luciferase Assay Buffer (Promega). Immediately after vortexing was complete, the luminescence intensity in relative light units (RLU) was measured using a luminometer (GloMax 20/20, Promega). The residual supernatant (1 μL) obtained from the lysate was diluted with Milli-Q water (5 μL). After the solution was mixed with Bradford Dye Reagent (Takara Bio, Inc., Shiga, Japan), the absorbance at 595 nm was measured by a SpectraMax iD3 Multi-Mode Microplate Reader (Molecular Devices Co., San Jose, CA) to quantify the protein concentration. The RLU values were obtained from 8 or 16 biologically independent samples and analyzed from 6 or 12 samples, in which the maximum and minimum values were removed as outliers. The RLU/mg value, in which the RLU value was divided by the protein amount, was calculated to evaluate the quantitative pDNA delivery efficiency.

## Results and discussion

### Synthesis and characterization of $(KUA)_3$-$(LU)_4$ peptide

A peptide-mimicking bZIP domain was developed to form a peptide/pDNA complex without strong electrostatic interactions. We synthesized peptide **1**, which contained $(LU)_4$ sequence, a leucine-rich sequence, and $(KUA)_3$ peptide, a cationic sequence (Fig. 1). To conjugate two peptides, the peptides were linked through two heterobifunctional cross-linking reagents. Therefore, the N-terminal amine of $(LU)_4$ **3** peptide was coupled with a thiol group of $(KUA)_3$ **2** cysteinyl peptide via sulfo-EMCSs, a cross-linking reagent composed of maleimide and succinimide (Supplementary Scheme S1). Boc-$(LU)_4$-OMe **3** was synthesized via liquid-phase synthesis as previously described [36, 37], while Ac-$C(KUA)_3$-$NH_2$ **2** was synthesized by solid-phase peptide synthesis (SPPS) (Supplementary Fig. S1). These peptides were cross-linked by sulfo-EMCSs and subsequently purified via HPLC to afford $(KUA)_3$-$(LU)_4$ **1** (26% isolated yield). The synthesized product was confirmed by MALDI-TOF MS and analytical HPLC (Supplementary Fig. S1).

The size and morphology of the peptide assemblies were evaluated by DLS and AFM, respectively. The formation of assemblies with a size of 226 ± 5 nm was confirmed by the average diameter obtained from the DLS measurements of $(KUA)_3$-$(LU)_4$ **1** peptide solution at 27 μM (Table 1). The AFM image of the peptide revealed the presence of spherical assemblies, and the sizes estimated by AFM corresponded to the hydrodynamic diameters determined by DLS (Fig. 2). In contrast, DLS measurements of $(KUA)_3$ **2** peptide solution revealed that uniformed assembly does not occur in the absence of the $(LU)_4$ sequence. It has been reported that in water, amphiphilic peptides composed of $(LU)_4$ and hydrophilic peptides form micelles with hydrophilic peptides on the outside [30]. These results suggest

**Table 1** Hydrodynamic diameters and PDIs of aqueous peptide solutions

| | Hydrodynamic diameter[a] (nm) | PDI[a] |
|---|---|---|
| $(KUA)_3$-$(LU)_4$ **1** | 226 ± 5 | 0.280 |
| $(KUA)_3$ **2** | 469 ± 107 | 0.454 |
| $(LU)_4$ **4** | 10.2 ± 2 | 0.448 |

[a]Values were determined by DLS measurements and are shown as the means ± standard deviations ($n = 3$)

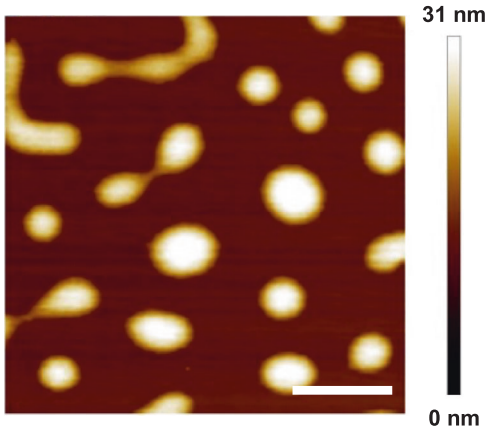


**Fig. 2** AFM image showing the assembly of $(KUA)_3$-$(LU)_4$ **1** on a cleaved mica substrate. The scale bar represents 500 nm. The color bar represents the height of the micelle

that peptide **1** formed a micelle in aqueous solution due to hydrophobic interactions with the $(LU)_4$ sequence.

## Preparation and characterization of peptide/pDNA complexes

An aqueous solution of $(KUA)_3$-$(LU)_4$ **1** or $(KUA)_3$ **2** was mixed with pDNA (p35S-NLuc-tNOS) to prepare peptide/pDNA complexes at various N/P ratios. The complexes were characterized through agarose gel electrophoresis, DLS, zeta potential measurements, and CD spectroscopy, and the morphological appearance of the peptide/pDNA complexes was studied via AFM. Agarose gel electrophoresis confirmed that complexes of peptides and pDNA formed, as indicated by a shift in DNA band at N/P = 5.0 in the mixture of pDNA and both peptides (Supplementary Fig. S2). Even for the mixtures of $(KUA)_3$ **2** and pDNA at N/P = 1.0, $(KUA)_3$ **2** interacted with pDNA, as the DNA bands underwent a mobility shift. The results indicated that the $(KUA)_3$ **2** functions as a DNA binding peptide. In contrast, for the mixture of $(KUA)_3$-$(LU)_4$ **1** and pDNA, the band density of the pDNA remained unchanged up to N/P = 5.0. This peptide assembles in an aqueous solution, suggesting that the interaction between the $(KUA)_3$ sequence and pDNA was weakened by steric hindrance. Conversely, compared to $(KUA)_3$ **2**, the $(KUA)_3$-$(LU)_4$ **1** complex was formed by a weaker interaction; in addition, this process is expected to facilitate DNA release from the complex.

**Table 2** Hydrodynamic diameters and PDIs of peptide/pDNA complexes prepared from $(KUA)_3$-$(LU)_4$ **1** or $(KUA)_3$ **2** peptides and pDNA (p35S-NLuc-tNOS) at various N/P ratios

| | $(KUA)_3$-$(LU)_4$ 1 /pDNA | | $(KUA)_3$ 2 /pDNA | |
|---|---|---|---|---|
| N/P ratio | Hydrodynamic diameter[a] (nm) | PDI[a] | Hydrodynamic diameter[a] (nm) | PDI[a] |
| 0.5 | 78.75 ± 3.8 | 0.351 | 308.2 ± 14 | 0.610 |
| 1.0 | 126.6 ± 4.9 | 0.355 | 264.7 ± 49 | 0.683 |
| 2.0 | 180.1 ± 3.2 | 0.272 | 107.9 ± 2.0 | 0.651 |
| 5.0 | 1557 ± 250 | 0.666 | 700.1 ± 14 | 0.236 |

[a]Values were determined by DLS measurements and are shown as the means ± standard deviations ($n = 3$)

According to DLS measurements, complexes with hydrodynamic diameters ranging from 79 to 180 nm were formed in mixtures of $(KUA)_3$-$(LU)_4$ **1** and pDNA at N/P = 0.5–2.0 (Table 2). These results indicate that $(KUA)_3$-$(LU)_4$ **1** condensed pDNA and complexes with an optimal size. Zeta potential measurements revealed that these complexes exhibited a negative charge (Supplementary Table S1). Even with a high abundance of positively charged peptide, the zeta potential of $(KUA)_3$-$(LU)_4$/pDNA complex was negative at N/P = 2.0, suggesting that the pDNA was present on the surface of the complexes. At N/P = 5.0, a complex larger than 1 μm was formed that exhibited a neutral charge, likely because the electrostatic repulsion between the complexes disappeared at N/P = 5.0. These results suggested that $(KUA)_3$-$(LU)_4$/pDNA complexes approximately 100 nm in size were stably formed in water at N/P = 0.5–2.0; these complexes formed due to the electrostatic repulsion generated by the negative charge of the DNA on the surface of the complex. On the other hand, in the case of $(KUA)_3$ **2**, complexes were formed with hydrodynamic diameters ranging from 100 to 300 nm in the presence of pDNA at N/P = 0.5–2.0. However, these complexes exhibited a PDI above 0.5. These results clarified that the $(LU)_4$ sequence was necessary to form a uniform complex.

The morphology of the peptide/pDNA complexes was confirmed by AFM observation. The AFM observations were carried out with pDNA (p35S-NLuc-tNOS), the $(KUA)_3$/pDNA complex, and the $(KUA)_3$-$(LU)_4$/pDNA complex at N/P = 1.0 on a cleaved mica surface under an ambient atmosphere. The AFM image of pDNA revealed a supercoiled structure that was approximately 500 nm in size (Fig. 3A-i). In contrast, an AFM image of $(KUA)_3$-$(LU)_4$ **1** combined with pDNA revealed spherical complexes with a diameter of approximately 200 nm without the supercoiled pDNA (Fig. 3A-ii). This image indicated that $(KUA)_3$-$(LU)_4$

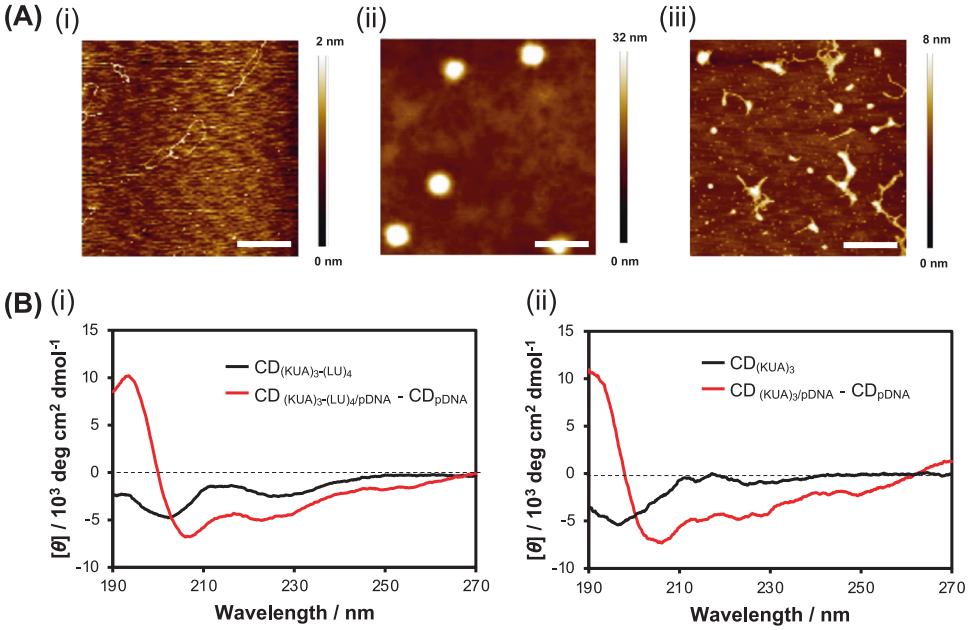


**Fig. 3** **A** AFM images of (i) pDNA only, (ii) the $(KUA)_3$-$(LU)_4$/pDNA complex at N/P = 1, and (iii) the $(KUA)_3$/pDNA complex at N/P = 1.0 on a cleaved mica substrate. Scale bars = 500 nm. The color bars represent the height of the complex. **B** (i) CD spectra of the aqueous solution of $(KUA)_3$-$(LU)_4$ **1** in the presence (red) and absence (black) of pDNA at N/P = 1. (ii) CD spectra of aqueous solutions of $(KUA)_3$ **2** in the presence (red) and absence (black) of pDNA at N/P = 1. The CD differential spectra (red) of peptide/pDNA complexes were obtained by subtracting the CD spectra of the pDNA from that of the peptide/pDNA complex

**1** condensed pDNA into spherical complexes. An AFM image of $(KUA)_3$ **2** combined with pDNA revealed the presence of amorphous complexes and spherical complexes with a size of approximately 100 nm (Fig. 3A-iii). These complexes corresponded to the Z-average and PDI obtained from DLS of $(KUA)_3$ **2** solution (Table 1). This image revealed that $(KUA)_3$ **2** alone was insufficient for condensing pDNA into complexes with optimal sizes for gene delivery. These results suggest that $(LU)_4$ sequences are necessary to form complexes suitable for gene delivery.

The CD spectra of peptide/pDNA complexes at an N/P ratio = 1.0 and peptide only were measured in aqueous solution (Milli-Q) to determine the secondary structures of the peptides (50 μM) in the complexes. The CD spectra of the peptides in mixed solutions were obtained by subtracting the CD spectrum of pDNA from the spectrum of mixed solutions to eliminate Cotton effects caused by pDNA (Supplementary Fig. S3). The CD spectra of $(KUA)_3$-$(LU)_4$ **1** and $(KUA)_3$ **2** without additives showed a random coil structure. However, in the presence of pDNA, the CD spectra of both peptides exhibited negative peaks at 226 and 208 nm and a positive peak at 193 nm, indicating that peptides **1** and **2** form α-helical conformations (Fig. 3B). Cell-penetrating peptides have been reported to adopt a more helical conformation in the presence of sodium dodecyl sulfate (SDS), an anionic surfactant [38]. Thus, the α-helical conformation of peptides **1** and **2** might be promoted in the presence of anionic pDNA. This result indicated that $(KUA)_3$-$(LU)_4$ **1** adopted a basic leucine zipper-like α-helical conformation similar to the natural bZIP domain despite its maleimide linkage; therefore, the ability of **1** to bind pDNA was confirmed.

Furthermore, the peptide can condense pDNA to approximately 130 nm, which is the optimal size for transfecting plant cells. However, pDNA condensation by $(KUA)_3$ **2**, which lacks $(LU)_4$ sequences, was incomplete; therefore, the leucine-rich $(LU)_4$ sequence may be essential for compact pDNA condensation. This effect may be driven by hydrophobic interactions between $(LU)_4$ sequences. In contrast, the interaction between $(KUA)_3$-$(LU)_4$ **1** and pDNA was weak, as demonstrated by the electrophoresis results. This weak interaction may result from the formation of assemblies by $(KUA)_3$-$(LU)_4$ **1** in water, which hinders the interaction between the cationic lysine residue of $(KUA)_3$ and pDNA due to steric hindrance. As this interaction weakens, the release of pDNA from peptide/pDNA complexes may become more robust.

## Introduction of peptide/pDNA and expression of protein in plant cells

Through CLSM observations and luciferase assays, we evaluated the ability of peptide/pDNA complexes to deliver pDNA in plant cells and rapidly release pDNA. In a previous study, a complex with a negative surface and a size of approximately 100 nm was introduced into plant cells because this complex is not trapped in the cell wall [8, 14]. Therefore, we prepared the complex at N/P = 1.0 and introduced it into intact leaves of *A. thaliana* using a needleless syringe [11]. For CLSM observation, Cy3-labeled pDNA (p35S-NLuc-tNOS) was complexed with peptides **1** and **2**. After 14 h of incubation, the leaves were stained with calcofluor white and subjected to CLSM (Supplementary Fig. S4). Z-stack images showed that Cy3 (red) generated

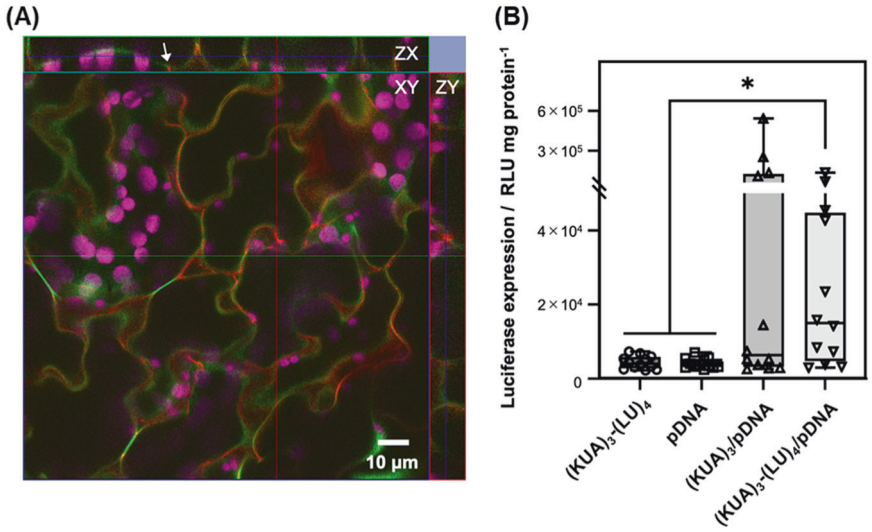


**Fig. 4** **A** Z-stacked CLSM image showing the internalization of the $(KUA)_3$-$(LU)_4$/Cy3-labeled pDNA complex (n/P = 1) into *A. thaliana* leaf cells. The XY plane shows a selected representative of 29 Z-stacked images. The green-framed image represents the ZX plane on the green line. The red-framed image represents the ZY plane on the red line. The leaf cell walls were stained with calcofluor white (green). The chlorophylls were visualized by their autofluorescence (magenta). The white arrow indicates that fluorescence from Cy3 (red) was observed in the leaf cell. **B** Transfection efficiency quantified by the levels of luciferase expression in *A. thaliana* leaves transfected with $(KUA)_3$-$(LU)_4$ **1** only, pDNA only, the $(KUA)_3$/pDNA complex or the $(KUA)_3$-$(LU)_4$/pDNA complex at N/P = 1. $P < 0.05$ (*) was considered to indicate statistical significance according to Dunnett's test ($n = 12$)

fluorescence from within the fluorescence of calcofluor white, indicating that $(KUA)_3$-$(LU)_4$(**1**)/Cy3-labeled pDNA complex was successfully introduced into the plant cell (Fig. 4A). Similarly, $(KUA)_3$(**2**)/Cy3-labeled pDNA complex was introduced to confirm that Cy3-labeled pDNA was present inside plant cells (Supplementary Fig. S5). These CLSM observations showed that both peptide/DNA complexes were introduced into the plant. Therefore, we performed a luciferase assay to evaluate the difference in the efficiency when pDNA is introduced into plant cells.

After peptide/pDNA complexes ($(KUA)_3$-$(LU)_4$ **1** or $(KUA)_3$ **2** and p35S-NLuc-tNOS) and two control samples (peptide only and pDNA only) were introduced into *A. thaliana* leaves, the transfection and expression of pDNA were evaluated using a Nano-Glo Luciferase assay. To analyze the dissociation profile of peptide/pDNA complexes, a time-course expression study was performed with the luciferase reporter and varying incubation times (4, 8, 16, and 24 h) after infiltration with peptide/pDNA complex solutions [39]. The statistical significance of the difference in expression was evaluated based on Dunnett's test, and after treatment with $(KUA)_3$-$(LU)_4$/pDNA complex, a significance level ($P < 0.01$) was obtained at 24 h (Supplementary Fig. S6). Therefore, we compared the RLU value of each sample at 24 h. Compared to the control samples, $(KUA)_3$-$(LU)_4$/pDNA complex at N/P = 1.0 showed a greater transfection efficiency, which confirmed that gene delivery and transfection were successful (Fig. 4B). On the other hand, in the case of $(KUA)_3$/pDNA complex, very high RLU values were found for some leaves; however, there was no significant difference compared to those of the control sample (Fig. 4B). To introduce pDNA into plant cells, the peptide/pDNA complex penetrates the cell wall and subsequently releases pDNA from the complex. Reportedly, the surface cationic charge and size of complex surfaces affect the efficiency of pDNA introduction [8, 14, 39]. In this study, pDNA and $(KUA)_3$-$(LU)_4$ **1** formed uniform complexes of approximately 130 nm, which is suitable for plant transfection. On the other hand, $(KUA)_3$ **2** formed larger aggregated complexes at the same N/P ratio. Consequently, compared to peptide **2**, peptide **1** showed higher transfection efficiency with less variation. In some cases, peptide **2** showed high transfection efficiency because heterogeneous small particles were present in the aggregates. In addition, based on the electrophoresis results, the interaction between $(KUA)_3$-$(LU)_4$ **1** and pDNA was weaker than that between $(KUA)_3$ **2**. Therefore, compared to $(KUA)_3$ **2**, $(KUA)_3$-$(LU)_4$ **1** is more efficient at releasing pDNA from the complex, possibly resulting in significantly greater expression levels in plant cells.

Regarding the speed of pDNA release, 24 h of protein expression was necessary using $(KUA)_3$-$(LU)_4$ **1**, which is longer than the time previously reported [8, 13, 40]. It is known that peptide/pDNA complexes release pDNA through cleaving cationic peptides by proteases in cells. Peptide **1** is composed of Aib, a noncanonical amino acid, and the enzymatic degradation of the $(KUA)_3$ DNA binding sequence appears to be slow. As a result, the speed of

pDNA release is reduced and a longer time is needed for protein expression.

## Conclusion

In this study, we developed a novel pDNA-transfected peptide, $(KUA)_3$-$(LU)_4$, which mimics the bZIP domain derived from a DNA-binding protein. The peptide can bind pDNA through lysine residues to form uniform nanoparticles, and this process is strongly supported by a leucine-rich coiled coil scaffold. The peptide/pDNA complex was successfully introduced into plant cells to express the protein encoded by the pDNA. Greater levels of protein expression were attained with $(KUA)_3$-$(LU)_4$ than $(KUA)_3$ peptide without the LU repeat sequence. These results indicate the high dissociation efficiency of $(KUA)_3$-$(LU)_4$. Therefore, peptides that mimic the bZIP domain are likely to be efficient in pDNA condensation and as carrier peptides. Our work provides new fundamental insights into CPPs that use the bZIP domain and will advance designs of nanocarriers based on peptides.

**Acknowledgements** The authors thank Ms. Karin Nishimura (Kyoto University) for her technical support with the MALDI-TOF-MS and ESI-MS measurements. This work was supported by JST-ERATO (grant number JPMJER1602), JST-COI-NEXT, and the MEXT Program: Data Creation and Utilization-Type Material Research and Development Project (grant number JPMXP1122714694) to K.N.

## Compliance with ethical standards

**Conflict of interest** The authors declare no competing interests.

**Publisher's note** Springer Nature remains neutral with regard to jurisdictional claims in published maps and institutional affiliations.



## References

1. Altpeter F, Springer NM, Bartley LE, Blechl AE, Brutnell TP, Citovsky V, et al. Advancing crop transformation in the era of genome editing. Plant Cell. 2016;28:1510–20.
2. Yin K, Gao C, Qiu JL. Progress and prospects in plant genome editing. Nat Plants. 2017;3:17107.
3. Potrykus I. Gene-transfer to cereals - an assessment. Bio-Technol. 1990;8:535–42.
4. Ahmar S, Mahmood T, Fiaz S, Mora-Poblete F, Shafique MS, Chattha MS, et al. Advantage of nanotechnology-based genome editing system and its application in crop improvement. Front Plant Sci. 2021;12:663849.
5. Zhang H, Demirer GS, Zhang H, Ye T, Goh NS, Aditham AJ, et al. DNA nanostructures coordinate gene silencing in mature plants. Proc Natl Acad Sci USA. 2019;116:7543–8.
6. Demirer GS, Zhang H, Matos JL, Goh NS, Cunningham FJ, Sung Y, et al. High aspect ratio nanomaterials enable delivery of functional genetic material without DNA integration in mature plants. Nat Nanotechnol. 2019;14:456–64.
7. Kwak SY, Lew TTS, Sweeney CJ, Koman VB, Wong MH, Bohmert-Tatarev K, et al. Chloroplast-selective gene delivery and expression in planta using chitosan-complexed single-walled carbon nanotube carriers. Nat Nanotechnol. 2019;14:447–55.
8. Lakshmanan M, Kodama Y, Yoshizumi T, Sudesh K, Numata K. Rapid and efficient gene delivery into plant cells using designed peptide carriers. Biomacromolecules. 2013;14:10–16.
9. Mäe M, Myrberg H, Jiang Y, Paves H, Valkna A, Langel Ü. Internalization of cell-penetrating peptides into tobacco protoplasts. Biochim Biophys Acta Biomembr. 2005;1669:101–7.
10. Chen CP, Chou JC, Liu BR, Chang M, Lee HJ. Transfection and expression of plasmid DNA in plant cells by an arginine-rich intracellular delivery peptide without protoplast preparation. FEBS Lett. 2007;581:1891–7.
11. Watanabe K, Odahara M, Miyamoto T, Numata K. Fusion peptide-based biomacromolecule delivery system for plant cells. ACS Biomater Sci Eng. 2021;7:2246–54.
12. Law SSY, Miyamoto T, Numata K. Organelle-targeted gene delivery in plants by nanomaterials. Chem Commun. 2023;59:7166–81.
13. Miyamoto T, Tsuchiya K, Numata K. Endosome-escaping micelle complexes dually equipped with cell-penetrating and endosome-disrupting peptides for efficient DNA delivery into intact plants. Nanoscale. 2021;13:5679–92.
14. Chuah JA, Yoshizumi T, Kodama Y, Numata K. Gene introduction into the mitochondria of arabidopsis thaliana via peptide-based carriers. Sci Rep. 2015;5:7751.
15. Yoshizumi T, Oikawa K, Chuah JA, Kodama Y, Numata K. Selective gene delivery for integrating exogenous DNA into plastid and mitochondrial genomes using peptide-DNA complexes. Biomacromolecules. 2018;19:1582–91.
16. Chen QR, Zhang L, Stass SA, Mixson AJ. Co-polymer of histidine and lysine markedly enhances transfection efficiency of liposomes. Gene Ther. 2000;7:1698–705.
17. Badosa E, Ferre R, Planas M, Feliu L, Besalú E, Cabrefiga J, et al. Library of linear undecapeptides with bactericidal activity against phytopathogenic bacteria. Peptides. 2007;28:2276–85.
18. Zhi D, Zhang S, Wang B, Zhao Y, Yang B, Yu S. Transfection efficiency of cationic lipids with different hydrophobic domains in gene delivery. Bioconjug Chem. 2010;21:563–77.
19. Schaffer DV, Fidelman NA, Dan N, Lauffenburger DA. Vector unpacking as a potential barrier for receptor-mediated polyplex gene delivery. Biotechnol Bioeng. 2000;67:598–606.
20. Grigsby CL, Leong KW. Balancing protection and release of DNA: tools to address a bottleneck of non-viral gene delivery. J R Soc Interface. 2010;7:67–82.
21. Chuah JA, Numata K. Stimulus-responsive peptide for effective delivery and release of DNA in plants. Biomacromolecules. 2018;19:1154–63.
22. Landschulz WH, Johnson PF, Mcknight SL. The leucine zipper - a hypothetical structure common to a new class of DNA-binding proteins. Science. 1988;240:1759–64.

23. Alber T. Structure of the leucine zipper. Curr Opin Genet Dev. 1992;2:205–10.
24. Deng Y, Liu J, Zheng Q, Li Q, Kallenbach NR, Lu M. A heterospecific leucine zipper tetramer. Chem Biol. 2008;15:908–19.
25. Ellenberger TE, Brandl CJ, Struhl K, Harrison SC. The GCN4 basic region leucine zipper binds DNA as a dimer of uninterrupted alpha helices: crystal structure of the protein-DNA complex. Cell. 1992;71:1223–37.
26. Tegoni M. De novo designed copper α-helical peptides: from design to function. Eur J Inorg Chem. 2014;13:2177–93.
27. Sang P, Shi Y, Wei L, Cai J. Helical sulfono-γ-AApeptides with predictable functions in protein recognition. RSC Chem Biol. 2022;3:805–14.
28. Demizu Y, Okitsu K, Yamashita H, Doi M, Misawa T, Oba M, et al. α-Helical structures of oligopeptides with an alternating l-Leu-Aib segment. Eur J Org Chem. 2016;2:2815–20.
29. Misawa T, Ohoka N, Oba M, Yamashita H, Tanaka M, Naito M, et al. Development of 2-aminoisobutyric acid (Aib)-rich cell-penetrating foldamers for efficient siRNA delivery. Chem Commun. 2019;55:7792–5.
30. Ueda M, Makino A, Imai T, Sugiyama J, Kimura S. Tubulation on peptide vesicles by phase-separation of a binary mixture of amphiphilic right-handed and left-handed helical peptides. Soft Matter. 2011;7:4143–6.
31. Kanzaki T, Horikawa Y, Makino A, Sugiyama J, Kimura S. Nanotube and three-way nanotube formation with nonionic amphiphilic block peptides. Macromol Biosci. 2008;8:1026–33.
32. Itagaki T, Uji H, Imai T, Kimura S. Sterical recognition at helix-helix interface of Leu-Aib-Based polypeptides with and without a GxxxG-motif. Langmuir. 2019;35:7249–54.
33. Terada K, Gimenez-Dejoz J, Miyagi Y, Oikawa K, Tsuchiya K, Numata K. Artificial cell-penetrating peptide containing periodic α-aminoisobutyric acid with long-term internalization efficiency in human and plant cells. ACS Biomater Sci Eng. 2020;6:3287–98.
34. Odahara M, Watanabe K, Kawasaki R, Tsuchiya K, Tateishi A, Motoda Y, et al. Nanoscale polyion complex vesicles for delivery of cargo proteins and Cas9 ribonucleoprotein complexes to plant cells. ACS Appl Nano Mater. 2021;4:5630–5.
35. Fujita S, Motoda Y, Kigawa T, Tsuchiya K, Numata K. Peptide-based polyion complex vesicles that deliver enzymes into intact plants to provide antibiotic resistance without genetic modification. Biomacromolecules. 2021;22:1080–90.
36. Kai M, Takeda K, Morita T, Kimura S. Distance dependence of long-range electron transfer through helical peptides. J Pep Sci. 2008;14:192–202.
37. Otoda K, Kitagawa Y, Kimura S, Imanishi Y. Chain length dependent transition of $3^{10}$- to α-helix of Boc-(Ala-Aib)N-OMe. Biopolymers. 1993;33:1337–45.
38. Lindberg M, Jarvet J, Langel U, Gräslund A. Secondary structure and position of the cell-penetrating peptide transportan in SDS micelles as determined by NMR. Biochemistry. 2001;40:3141–9.
39. Miyamoto T, Tsuchiya K, Toyooka K, Goto Y, Tateishi A, Numata K. Relaxation of the plant cell wall barrier via zwitterionic liquid pretreatment for micelle-complex-mediated DNA delivery to specific plant organelles. Angew Chem Int Ed. 2022;61:e202204234.
40. Law SSY, Liou G, Nagai Y, Giménez-Dejoz J, Tateishi A, Tsuchiya K, et al. Polymer-coated carbon nanotube hybrids with functional peptides for gene delivery into plant mitochondria. Nat Commun. 2022;13:2417.